

Human sensing receiver for 802.11ax Wireless LAN

Ogechukwu Kanu

Dept. of Electrical and Software Engineering
ogechukwu.kanu@ucalgary.ca

Abstract—We present a direct conversion receiver architecture tailored for the IEEE 802.11ax standard (Wi-Fi 6) to enable efficient channel state information (CSI)-based sensing applications. By leveraging the inherent properties of Wi-Fi 6, our proposed design meets the stringent performance requirements for high-efficiency receivers, including sensitivity, selectivity, and interference rejection. This work addresses key challenges in integrating communication and sensing capabilities within the physical layer, offering a compact and cost-effective solution for next-generation applications such as smart environments and human activity recognition.

Index Terms—WiFi-Sensing, 802.11ax, Direct-Conversion, Zero-IF

I. INTRODUCTION

Next-generation mobile communication network (ie. 6G) has envisioned a network beyond communication functionality which will provide integrated sensing and communication (ISAC) capabilities. This will enable more emerging applications such as smart cities, connected vehicles, artificial intelligence of things (AIoT) and health care/elder care. In the last decade, significant progress has been made to employ massive wireless communication systems such as WiFi/4G/5G for human and environment sensing. Major efforts have been devoted to develop wireless sensing theories and techniques using channel state information (CSI) for both WiFi and 4G/6G networks due to their ubiquitous deployment, a lot of prototype applications ranging from vital sign monitoring, human-computer interaction, human activity recognition, to indoor localization and tracking have been built in both industry and academia

WiFi technology operates across multiple frequency bands, sub-7 GHz (including 2.4 GHz, 5 GHz and 6 GHz) and 60 GHz bands. There is widespread global adoption of these frequencies predominantly operating within the sub-7 GHz range by WiFi routers and IoT devices (including those compliant with IEEE 802.11n/ac/ax/be, or WiFi 4/5/6/7). WiFi sensing leverages the standard physical layer (PHY) of WiFi for both sensing measurements as well as digital communication. Since the PHY has been designed for communications, sensing operations must rely on the normal transmissions as defined by the 802.11 standard [1].

In an attempt to raise awareness and foster industry engagement, the Wireless Broadband Alliance (WBA) body established a WiFi Sensing Work Group. Through an exhaustive work on the potential of WiFi Sensing, presented a formal proposal to the IEEE with the aim of establishing standardized protocols for WiFi Sensing. Consequently, the approval for

IEEE 802.11bf project was granted by IEEE Standards Association which focuses on Wireless Local Area Network (WLAN) Sensing standardization. In the meantime, researchers have explored the potential of IEEE 802.11ax standard, also known as WiFi 6, in human sensing. For instance, studies have utilized 802.11ax's CSI to detect human activities, such as walking or running, by analysing how human motion affects WiFi signals

This work presents the proposed PHY design that satisfies the requirements of a high-efficient (HE) receiver according to the IEEE 802.11ax standard for sensing applications with CSI. In Section II, we discuss the design criteria for a HE PHY layer highlighting sensitivity and selectivity requirements. We propose a direct conversion architecture design and outline our justifications. Then in Section III, we present our lineup model and the corresponding calculated analysis. We compare our simulated analysis along with all analysis tests required by the standard in Section IV.

II. IEEE 802.11AX PHY SPECIFICATION

According to IEEE 802.11ax clause 4, the HE station (STA) operates in frequency bands between 1 GHz and 7.125 GHz. In the 5 GHz and 6 GHz bands for very high transmission (VHT) application, the STA supports the Orthogonal Frequency Division Multiplexing (OFDM) PHY as defined in clause 17 in 20 MHz (mandatory), 40 MHz, 80 MHz, and 160 MHz contiguous channel widths, and 80+80 MHz noncontiguous channel width.

In clause 27, the maximum number of users supported for downlink (DL) multi-user multiple input multiple output (MU-MIMO) transmissions is 8 users per resource unit (RU)

The general receiver specification specified by the standard considers the receiver minimum input sensitivity, the adjacent channel rejection, the non-adjacent interference rejection, the receiver maximum input level and the clean channel assessment (CCA) sensitivity. For the receiver design, we will consider all the specifications except the CCA which is beyond the scope. The input levels specified in the specification are considered as the average power per receive antenna.

A. Receiver minimum input sensitivity

The maximum packet error rate (PER) is **10%** for a physical layer service data unit (PSDU) with the rate-dependent input level stated in subclause 27.3.20.2. We consider a receiver channel bandwidth of **80 MHz** operating with **QPSK** modulation and **1/2** code rate without dual carrier modulation (DCM) at **-73 dBm**.

B. Adjacent Channel Rejection

The adjacent channel rejection test applies to different bandwidths W MHz (where W is 20, 40, 80, or 160). It is measured by setting the desired signal's strength **3dB** above the rate-dependent sensitivity and setting the power of the interfering signal of W MHz bandwidth until 10% PER is caused for a PSDU of 4096 octets of QPSK modulation. *The corresponding adjacent channel rejection is the difference between the power of signals in the interfering channel and the desired channel.*

C. Nonadjacent Channel Rejection

The nonadjacent channel rejection test applies to different bandwidths W MHz (where W is 20, 40, 80, or 160). It is measured by setting the desired signal's strength **3dB** above the rate-dependent sensitivity and setting the power of the interfering signal of W MHz bandwidth until 10% PER is caused for a PSDU of 4096 octets of QPSK modulation. *The corresponding nonadjacent channel rejection is the difference between the power of signals in the interfering channel and the desired channel. The nonadjacent channel rejection shall be met with any nonadjacent channels located at least $2 \times W$ MHz away from the centre frequency of the desired signal.*

The corresponding rejection for the chosen rate-dependent input level are **13 dB** and **29 dB** for adjacent channel and non-adjacent channel respectively.

D. Receiver maximum input level

The maximum input level that provides a maximum PER of 10% at the PSDU length of 4096 octets for QPSK modulation in is **-30dBm** 5GHz band.

TABLE I
RECEIVER SPECIFICATION DESIGN

Receive band	Channel 155
Signal/Channel bandwidth	80MHz
Sensitivity (S_{min})	-73dBm
Maximum Input level (S_{max})	-30dBm
PER	10%
Minimum desired received signal power (S_d)	$S_{min} + 3$
Power of adjacent interferers (I_{adj})	$S_d + 13$
Power of nonadjacent interferers (I_{nadj})	$S_d + 29$
Power of out of band interferers (I_{out})	0dBm ¹

E. Down conversion architecture

For these design requirements, we are choosing a direct conversion (zero-IF) architecture for the following reasons. For cost-sensitive and power-constrained applications, direct conversion is a preferred choice because it avoids two or more stages of conversion which leads to fewer components. Consequently, it is preferable for applications with stringent size constraints. However, despite overall reduction in complexity and parts count, the direct conversion introduces the problem of unwanted baseband signals as a tone at any frequency can generate a 2nd order nonlinearity at DC. However, with the OFDMA configuration in 802.11ax the distortions from DC can be avoided by transmitting in all subcarriers besides the DC.

III. DESIGN CONSIDERATIONS FOR DIRECT CONVERSION I/Q RECEIVER

As highlighted in the previous section, direct conversion has a few sets of implementation complications. One of which is the presence of unwanted baseband signals generated by 2nd order nonlinearity of the receiver. In this section, we analyse the distortion budget of a typical direct conversion receiver considering only the first stage of conversion. Figure 1 is the block diagram of a typical WiFi 802.11ax receiver with some key characteristics as follows:

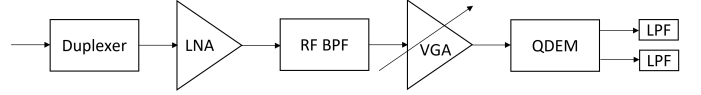


Fig. 1. Typical Direct conversion block diagram showing one down conversion stage

Receive band: 5.735 GHz to 5.815 GHz (for channel 155)
Channel Bandwidth: 80 MHz
Number of carriers: 4

A. Receiver Noise Figure and Distortion budget

With the given receiver specifications given in Table I, we can calculate the receiver noise figure and distortion budget. The acceptable PER is 10% and the minimum carrier-to-noise ratio (CNR_{min}) can be calculated for QPSK modulation as approximately **3dB**.

First we calculate the maximum noise figure, NF_{rx_max} of the receiver as follows

$$N_{floor} = -174dB/Hz + 10 \times \log(BW) + NF_{rx_max}$$

$$\text{Also, } N_{floor} = S_{min} - CNR_{min}$$

$$\text{Thus, } NF_{rx_max} = S_{min} - CNR_{min} + 174 - 10 \times \log(8 \times 10^7)$$

$$NF_{rx_max} = \mathbf{18.96 \text{ dB}}$$

Next, we calculate the distortion budget for the components of the receiver for allowable signal degradation.

$$\begin{aligned} \text{Maximum Degradation, } D_{max} &= S_d - CNR_{min} \\ &= \mathbf{-73.01dB} \end{aligned}$$

Allowable Degradation/Distortion,

$$\begin{aligned} D_{a_dBm} &= 10 \times \log \left(10^{\frac{D_{max}}{10}} - 10^{\frac{N_{floor}}{10}} \right) \\ &= \mathbf{-76.03dBm} \end{aligned}$$

The distortion budget for the receiver maximizes the intermodulation distortion (IMD) of the quadrature demodulator particularly the 2nd order IMD (IMD2). In addition, the OFDM modulation is used and allows for reduced degradation from DC offset and flicker noise by avoiding the centre subcarrier, thus the main sources of distortions are *the IMD2 generated by the second-order non-linearity of the quadrature demodulator, IMD3 generated by the third-order non-linearity of the quadrature demodulator, and the phase noise distortion, P_{phn} , and phase spurs, P_{spur} , generated by mixing the local*

oscillator phase noise, N_{phase} , and N_{spur} , with the interferes in the quadrature demodulator.

$$P_{IM2_max} = 0.475 \times D_a$$

$$P_{IM3_max} = 0.2375 \times D_a$$

$$P_{phn} = 0.11875 \times D_a$$

$$P_{spur} = 0.11875 \times D_a$$

$$\text{Other distortions} = 0.05 \times D_a$$

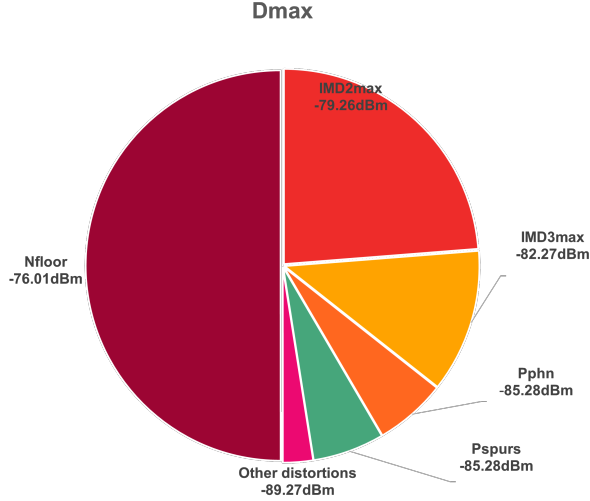


Fig. 2. Distortion Budget for Direct conversion receiver

The calculated distortion budget can be visualized in Figure 2 and the maximum distortion across the main sources of distortion are as follows:

$$IMD2_{max} = -79.26 \text{ dBm}$$

$$IMD3_{max} = -82.28 \text{ dBm}$$

$$P_{phn_dBm} = -85.28 \text{ dBm}$$

$$P_{spur_dBm} = -85.28 \text{ dBm}$$

$$\text{Other distortions} = -89.04 \text{ dBm}$$

With the power budget for the different sources of distortions let us select our components.

B. Component Selection

Let's choose components such that the gain and noise figure are satisfied. The first element in the lineup as shown in Figure 1 is the duplexer. A requirement for the element is high selectivity and low noise figure as it significantly affects the overall noise figure of the receiver. A typical value for the insertion loss ~ 1 dB. The next component in the lineup is the low noise amplifier (LNA). A typical component for wireless receiver applications in the 5 GHz to 6 GHz band is the BGU7258 low-noise amplifier MMIC with the following specifications:

```

1 Frequency of operation f: 5.5 GHz
2 Power gain Max @ 5.9 GHz: 16 dB
3 Input power at 1dB compression: -4 dBm
4 Noise Figure: 1.6 dB
5 IIP3: 27 dBm (two-tone at 5MHz spacing)

```

Next, we select the RF bandpass filter. The component specification requirements are 5 GHz operating band with ~ 80 MHz of bandwidth and insertion loss of < 2 dB with high rejection in out-of-bands. For this component, we chose the QPQ1904 Wi-Fi bandBoost Bulk Acoustic Wave (BAW) filter. It exhibits a low loss in the Wi-Fi UNII2c-3 band and high near-in rejection in the UNII1-2a band. The specification of the QPQ1904 component is given as follows:

```

1 Receive band: 5490 MHz - 5835 MHz
2 Insertion loss in UNII2c-3: 1.6 dB
3 Rejection in UNII1-2a bands (@f = 5170 - 5330 MHz): 55 dB

```

For the variable gain amplifier (VGA) we select a component that gives a power level of **-40dBm** for the desired signal at the end of the lineup. It considers the maximum input level S_{max} , such that an attenuation of -10 dB is needed in the lineup to achieve a power level of -40 dBm. The component of choice in the selected band of operation is MAAM-011100 with a range of -20 dB to 10 dB at 5 dB noise figure. The component specifications are as follows:

```

1 Frequency band: 400 MHz to 20 GHz
2 Gain range: -20 dB to 10 dB
3 Noise Figure @ maximum gain: 5 dB
4 Input power at 1dB compression point @ 10 GHz: 15 dBm
5 IIP3: 15dBm

```

The most important component in the lineup is the quadrature demodulator. Assuming all of the intermodulation distortions occur at this component then the IIP2 and IIP3 need to be as high as possible to meet the maximum degradation allowed. We selected the LTC5586 6GHz high linearity I/Q demodulator optimized for zero-IF and low-IF designs. It has a high OIP2 of up to 80 dBm and a conversion gain of 7.7 dB. The component specifications are as follows:

```

1 Frequency band: 300 MHz to 6 GHz
2 Conversion gain @ 5800 MHz: 0.7 dB
3 Noise Figure @ 5800 MHz: 31 dB
4 OIP2 @ 5800 MHz: 49/56 dBm
5 OIP3 @ 5800 MHz: 32/33 dBm
6 Output 1dB compression point @ 5800 MHz: 12.5 dBm
7 LO to RF Leakage @ 5800 MHz: -47 dBm
8 RF to LO isolation @ 5800 MHz: 52 dB
9 RF to IF isolation @ 5800 MHz: 47 dB
10 LO to IF leakage @ 5800 MHz: -36dBm

```

The last component in the lineup is the low-pass filter. Typical value for the insertion loss that operates within 80 MHz of bandwidth is 3 dB.

IV. RESULT AND DISCUSSION

This section is dedicated to the results obtained from Keysight Advanced Design Simulation (ADS) software. We simulate the noise figure of the lineup and carry out two tests; adjacent and nonadjacent interference rejection.

A. Receiver Noise Figure

With the selected components, we simulate the nonlinear noise figure with harmonic balance simulation for different input signal power from -70dBm to 10dBm as shown in Figure 3. The small-signal noise figure is **8.857** dB as indicated by the marker. Using Friis formula, we calculate the equivalent noise figure as follows:

$$F_{eq} = F_1 + \frac{F_2 - 1}{g_1} + \frac{F_3 - 1}{g_1 g_2} + \frac{F_4 - 1}{g_1 g_2 g_3} + \frac{F_5 - 1}{g_1 g_2 g_3 g_4} + \frac{F_6 - 1}{g_1 g_2 g_3 g_4 g_5}$$

$$NF_{eq} = 10 \times \log(F_{eq}) = \mathbf{8.86dB}$$

We observe that the calculated value corresponds to the simulated value. Additionally, we run an envelope simulation with the signal at the desired signal input power of -70dB at the input of the receiver with no interference observing the SNR at the end of the lineup with and without intermodulation distortions from the components. The values are shown in Figure 4 and 5. The simulated SNR values are **15.691dB** and **15.721dB** respectively and they satisfy the minimum required CNR, CNR_{min} , for the receiver. The calculated SNR due to noise contribution alone is $S_o - N_o = -48.9\text{dBm} - (-65.01\text{dBm}) = \mathbf{16.11dB}$.

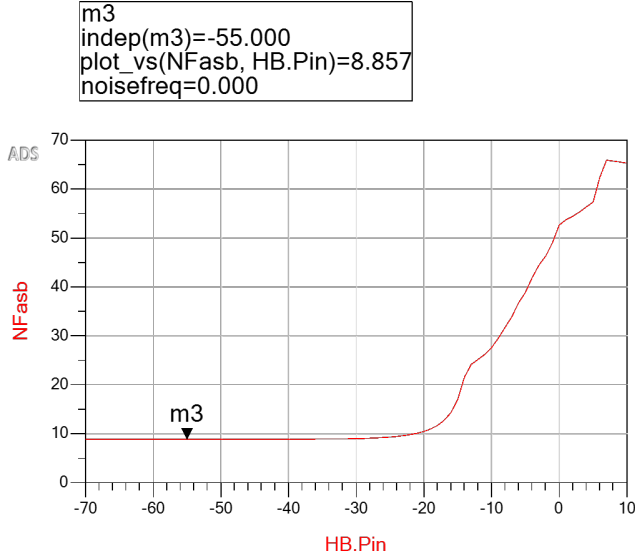


Fig. 3. Nonlinear noise analysis of the receiver for different input power to the receiver

P_signal_dBm	P_error_dBm	SNR_dB
-57.661	-73.351	15.691

Fig. 4. SNR at the end of the lineup without intermodulation distortion

P_signal_dBm	P_error_dBm	SNR_dB
-57.647	-73.368	15.721

Fig. 5. SNR at the end of the lineup with intermodulation distortion

Figures 6 and 7 show the spectrum plot of the signal at the input and output of the receiver. We simulate a single subcarrier of 312.5kHz in the 80MHz band offset from DC to avoid any distortions from DC offset and flicker noise.

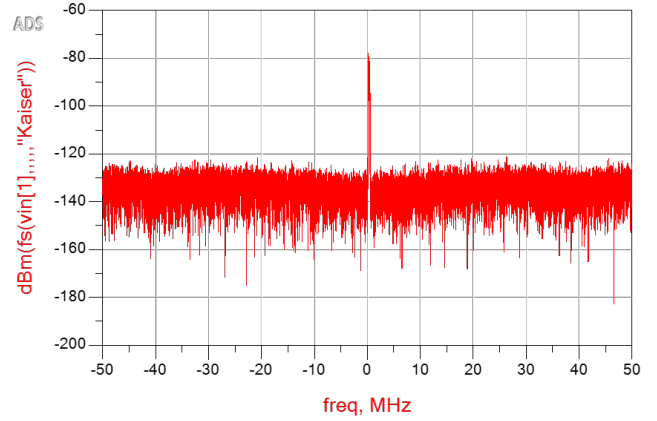


Fig. 6. Spectrum of the desired signal at the input of the receiver

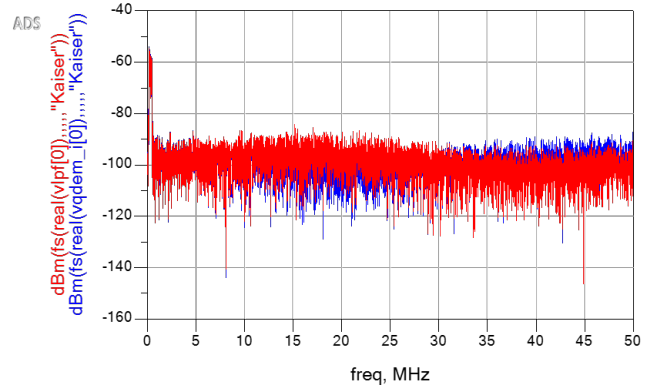


Fig. 7. Spectrum of signal at the output of the receiver for the in-phase line. Blue plot is the output of the quadrature demodulator while the red plot is the output of the low-pass filter

B. Adjacent Interference Rejection

For the adjacent interference rejection test, we set the power of the interference in the adjacent channel at $S_d + 13\text{dB}$ and measure the SNR at the end of the lineup. Figures 8 and 9 show the signals at the input and output of the receiver. The plot shows the desired signal and the interferer of bandwidth, 80MHz.

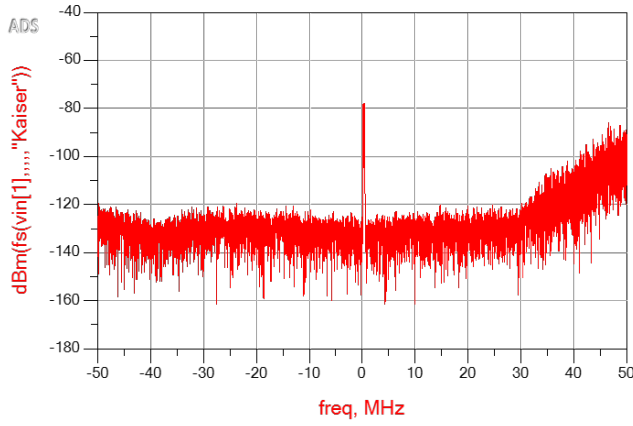


Fig. 8. Spectrum of signals at the input of the receiver for adjacent interference test

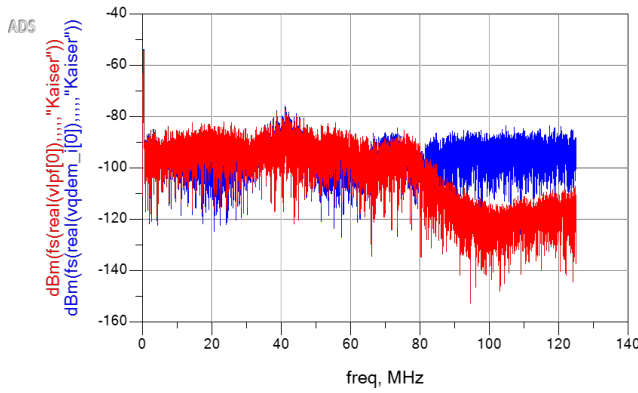


Fig. 9. Spectrum of signals at the output of the receiver for adjacent interference test

The simulated SNR at the output of the receiver is given in Figure 10. It is measured as **13.191 dB** which is above the minimum CNR, CNR_{min} . This is because, with the high second-order and third-order intercept points, IIP2, and IIP3, for the components, the maximum allowable distortion is satisfied. We can verify this conclusion by calculating the minimum IIPs if all of the intermodulation distortion occurs at the quadrature demodulator as follows:

Recall,

$$IMD2_{max} = -79.26 \text{ dBm}$$

$$IMD3_{max} = -82.28 \text{ dBm}$$

$$IIPm = m \times I_{in} - (m - 1)IMDm$$

At the input of the quadrature demodulator, the interference power is $I_{in} + G = -33.6\text{dBm}$. Thus the minimum IIPs are

P_signal_dBm	P_error_dBm	SNR_dB
-57.817	-71.008	13.191

Fig. 10. SNR at the end of the lineup with adjacent interferer at $S_d + 13\text{dB}$

calculated as follows:

$$IIP2_{min} = 2 \times I_{in} - IMD2_{max} = \mathbf{12.06\text{dBm}}$$

$$IIP3_{min} = \frac{3 \times I_{in} - IMD3_{max}}{2} = \mathbf{-9.26\text{dBm}}$$

The minimum values of OIPs given the gain of the quadrature demodulator, 0.7dB, are **12.76 dBm** and **-8.56 dBm** for the OIP2 and OIP3 respectively. The values of the OIPs in the quadrature modulator over satisfies the requirements.

V. CONCLUSION

We have successfully designed a direct conversion receiver for the Wi-Fi 802.11ax standard for CSI-based human sensing in a 80MHz band channel that satisfies the PER requirements of 10% at the output of the receiver for a QPSK modulation at 1/2 code rate in OFDMA configuration and passes the adjacent interference rejection test. The project has shown the importance of a good architecture design for the given requirements and good component selection.

Though not covered in the project results, we expect similar performance of the receiver with the nonadjacent interference test where it shows a good CNR measurement compared to the minimum requirement. In addition, the project can benefit from investigating the impact of the frequency leakage, oscillator phase noise and spurs in the quadrature demodulator. We hope to investigate further in the future.

REFERENCES

- [1] *IEEE Standard for Information Technology–Telecommunications and Information Exchange between Systems Local and Metropolitan Area Networks–Specific Requirements Part 11: Wireless LAN Medium Access Control (MAC) and Physical Layer (PHY) Specifications Amendment 1: Enhancements for High-Efficiency WLAN*, Std., 2021, accessed: 2024-12-24. [Online]. Available: <https://ieeexplore.ieee.org/document/9442429>